Microwave Detection Using the Resonant Tunneling Diode

JOSEPH M. GERING, STUDENT MEMBER, IEEE, THOMAS J. RUDNICK, AND PAUL D. COLEMAN, LIFE FELLOW, IEEE

Abstract—**A detailed experimental and theoretical study in the use of a resonant tunneling diode (RTD) as a microwave detector based upon its small-signal equivalent circuit model is presented. It is shown that the rectified current from the diode can be accurately predicted and that the diode can be operated as a reactive microwave detector which absorbs no microwave power. For this detection mode, a matching network which maximizes the applied ac voltage can be used.**

I. INTRODUCTION

IN 1973 Tsu and Esaki [1] first proposed resonant tunneling (RT) in double barrier quantum well devices. By 1974 Chang, Esaki, and Tsu [2] had demonstrated that these devices have a negative differential resistance (NDR) region in their dc current–voltage (I–V) curves. However, the study of these diodes was slow until Sollner *et al.* [3] demonstrated their detection capabilities up to 2.5 THz in 1983. This exhibition of their high frequency response quickly stimulated further study of the RT diodes. In 1985 Shewchuk *et al.* [4] obtained room-temperature oscillations with a resonant tunneling diode (RTD). Coon and Liu [5] predicted a theoretical oscillation frequency limit of 1 THz in 1986. Gering *et al.* [6] presented a microwave circuit model for the RTD, and Sollner *et al.* [7] studied RTD oscillations up to 200 GHz in 1987. Recently, in a more detailed theoretical analysis, Frensley [8] has predicted that the NDR of the RTD should persist to 5 THz and that the nonlinearity should persist to 10 THz. The microwave circuit modeling of Gering *et al.* [6] now makes it possible to calculate the detailed behavior of an RTD as a microwave detector and compare the results with experiment. This paper describes RTD detector studies from 1 GHz to 10 GHz.

Passive detectors, like Schottky barrier diodes, must absorb power to operate. In an appropriately biased NDR diode, however, the negative resistance can cancel the device's positive resistance, leaving the net impedance of the diode purely reactive. For this case, while an RF voltage is across the diode, no net power is absorbed, and the diode detects the microwave voltage across the RTD.

Manuscript received November 16, 1987; revised February 1, 1988. This work was supported by the National Science Foundation under Grant ECS 84-13680 and by the McDonnell–Douglas Corporation Independent Research and Development Program.

The authors are with the Electro-Physics Laboratory of the Department of Electrical and Computer Engineering at the University of Illinois, Urbana, IL 61801-2991.

IEEE Log Number 8821215.

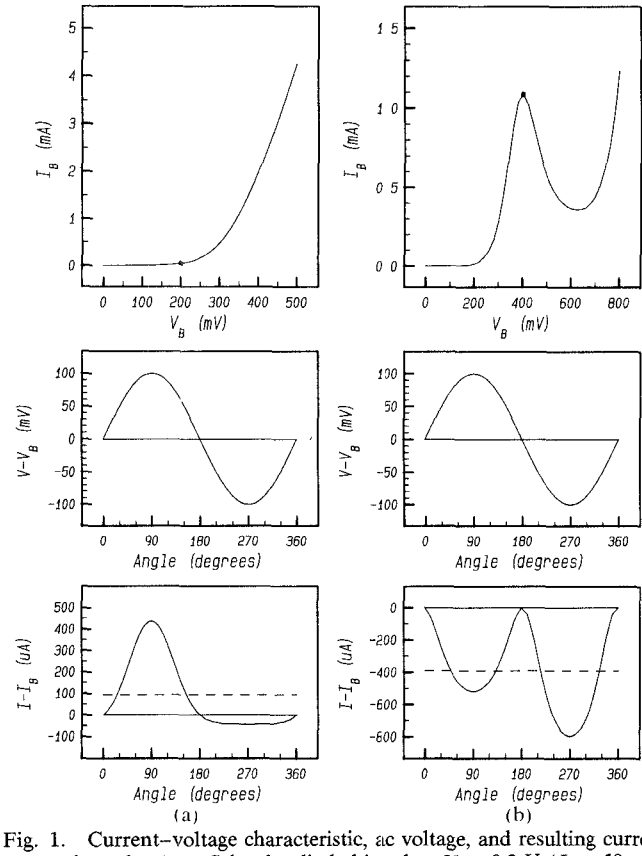

Fig. 1. Current–voltage characteristic, ac voltage, and resulting current waveform for (a) a Schottky diode biased at $V_B = 0.2$ V ($I_B = 50$ μA) and (b) a resonant tunneling diode biased at $V_B = 0.4$ V ($I_B = 1.086$ mA). The dashed line indicates the rectified current.

The impedance matching problem then reduces to inserting a transformer between the source and diode and adjusting the transformer toward the oscillation condition to obtain a regenerative detector [9]. This procedure has produced very sensitive detection with the Esaki tunnel diode [10]. Since the RTD has a smaller parasitic capacitance than the Esaki tunnel diode, the RTD should have a much higher cutoff frequency.

The detection properties of a diode depend on the nonlinear characteristics of its I–V curve. A passive detector, like a Schottky diode, only partially rectifies an applied ac signal (see Fig. 1(a)) while an RTD biased at its resonance peak acts as a full-wave rectifier (see Fig. 1(b)). This full-wave rectification ability plus the RTD's intrinsic speed make it an attractive candidate as a detector and mixer at high frequencies.

0018-9480/88/0700-1145$01.00 ©1988 IEEE

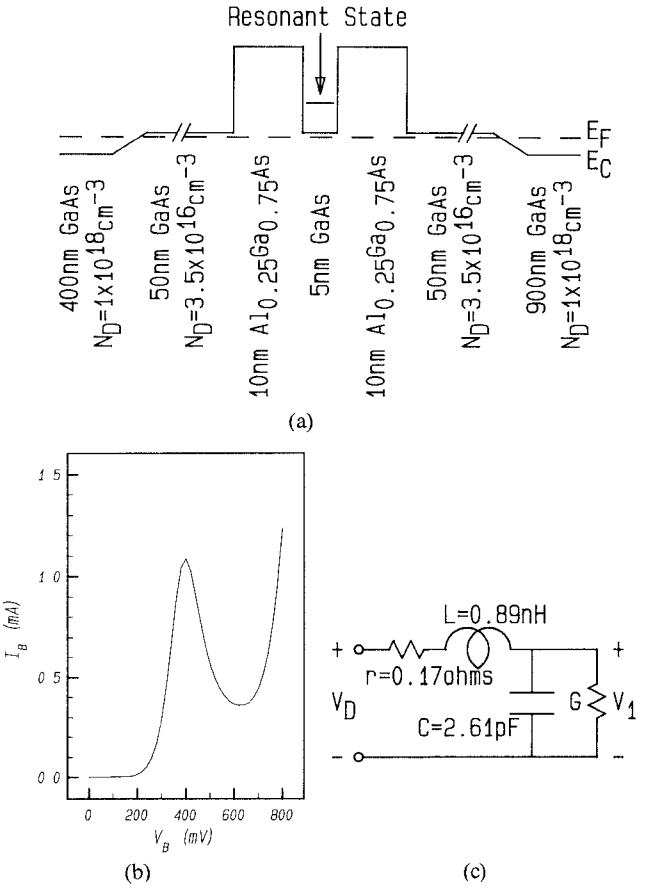

Fig. 2. (a) Conduction band diagram of the resonant tunneling diode giving the layer thicknesses and doping. (b) Current–voltage characteristic of the resonant tunneling diode (c) Resonant tunneling diode's equivalent circuit model.

II. Resonant Tunneling Diode Characteristics

The RTD used for this study was grown by molecular beam epitaxy using AlGaAs. Circular mesas of 50 μm diameter were etched from the completed wafer and ohmic contacts were made to the top and bottom of the structure. The wafers were diced and the individual diodes were bonded into C-3 microwave packages capped with C-11 lids [6], [11]. The diode's structure, doping levels, layer thicknesses, and conduction band diagram are shown in Fig. 2(a). Fig. 2(b) shows the diode's dc $I-V$ characteristic at 77 K, in which the NDR region extends from 0.4 V to 0.625 V. Sollner's [3] detector studies show that the nonlinearity of the $I-V$ curve persists from dc to at least 2.5 THz.

The lumped element microwave circuit model of the RTD [6] is shown in Fig. 2(c). It has essentially the same form as the model for an Esaki tunnel diode [12]. The model has a series resistance, r, a series inductor, L, and a nonlinear conductance, G, shunted by a capacitor, C. From [6], the parasitic elements (r, C, and L) were found to be independent of bias voltage, and for small signals, the active element (G) was given by the differential conductance of the dc $I-V$ curve. The series inductance which was introduced in [6] is a new feature of this device. In his theoretical analysis, Frensley [8] does predict an inductive effect in the resonant tunneling mechanism. However, Frensley's inductance is several orders of magnitude smaller than the series inductance of the RTD circuit model. The series inductance of the circuit model is probably caused by more circuit-related phenomena such as contact inductance, the electrical length of the semiconductor substrate, and inaccuracies in de-embedding the RTD impedance from the package at higher microwave frequencies. Recent preliminary measurements of an RTD bonded in a coplanar waveguide support this belief by yielding smaller inductances than those obtained for devices in the C-3 package.

Assuming the conductance persists throughout the microwave range and with a small series resistance ($r = 0.17$ Ω), the large-signal ac conductance, G_{ac}, can be found from the $I-V$ curve of the diode. At a given dc bias voltage, V_B, and with an ac voltage across the conductance of $V_1\cos(\omega t)$, the resulting current waveform can be determined from the $I-V$ curve. The current waveform can then be Fourier analyzed numerically to find its dc component, I_0, and its fundamental ac component, $I_1\cos(\omega t)$. The ac conductance is defined as

$$G_{ac} = I_1/V_1 = G_{ac}(V_B, V_1). \tag{1}$$

Although the use of a single frequency sinusoidal voltage is an approximation that assumes that the detector is a short at all of the harmonic frequencies, it will be shown that this assumption provides excellent agreement.

III. Microwave Detection

The detector measurements were performed with the equipment arrangement shown in Fig. 3(a). Source power settings of 1, 10, 100, and 1000 μW, with frequency settings of 1, 2, 3, 4, 7, and 10 GHz, were applied to the circuit. A representative sample of the measured rectified current of the detector from these settings is displayed in Fig. 3(b) and (c). Note that the greatest value for the magnitude of the rectified current appears at the resonance peak voltage ($V_B = 0.4$ V), where the full-wave rectification demonstrated in Fig. 1(b) occurs.

Between the signal source and the diode is a complicated circuit which consists of cables, a bias tee, adapters, and the C-3 package, but the entire circuit can be modeled by its S parameters [13], which were measured for this network. Then, the ac power, P_D, absorbed by the diode can be found from the following expression:

$$P_D = P_g\left[1-|\Gamma|^2\right]|S_{21}/(1-\Gamma S_{22})^2 \tag{2}$$

where P_g is the generator power and Γ is the complex reflection coefficient of the RTD. The voltage across the diode, V_D, is given by

$$V_D^2 = 2P_D|Z_D|^2/\mathrm{Re}(Z_D) \tag{3}$$

and the ac voltage, V_1, across the conductance, G, is related to V_D by

$$V_1 = V_D/|1+(r+j\omega L)(G_{ac}+j\omega C)|. \tag{4}$$

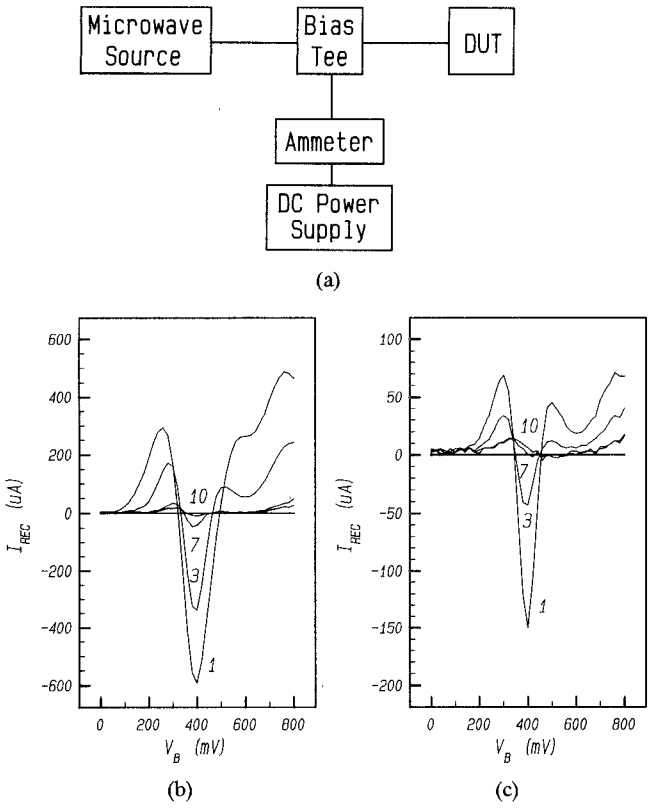

Fig. 3. (a) Equipment setup for the detector measurement. (b) Rectified current for a generator power of 100 μW. (c) Rectified current for a generator power of 10 μW. The different curves in parts (b) and (c) are labeled with their frequencies in GHz.

The diode impedance, Z_D, is given by the expression

$$Z_D = \left[r + \frac{G_{ac}}{G_{ac}^2 + (\omega C)^2} \right] + j \left[\omega L - \frac{\omega C}{G_{ac}^2 + (\omega C)^2} \right]. \quad (5)$$

The numerical Fourier analysis of the resulting current waveform with an applied sinusoidal voltage yields its dc component, I_0, from which the rectified current can easily be found by subtracting the zero incident power bias current, I_B. The rectified current, I_{REC}, can then be expressed as a function of the generator power through (2), (3), and (4).

Four comparisons of experimental and calculated values for I_{REC} versus V_B are shown in Fig. 4. The source power is 100 μW in these cases. The agreement between the measurements and the calculated curve at 1 and 3 GHz is excellent for most bias voltages. The errors at the high bias voltages could be attributed to slight nonlinearities in the shunt capacitance (C) at these voltages. Although one might expect some error to be caused by neglecting the harmonic frequencies in our analysis, in the next section we show that the effect of harmonic voltages and currents is negligible. (Neglecting harmonics would have a greater effect at lower fundamental frequencies, where the impedances of the parasitic elements at the harmonic frequencies would have less of an effect on the conductance.) For the 7 and 10 GHz cases, the experimental and calculated data show a greater spread in values. The rectified current decreases with frequency since the conductance (G) is

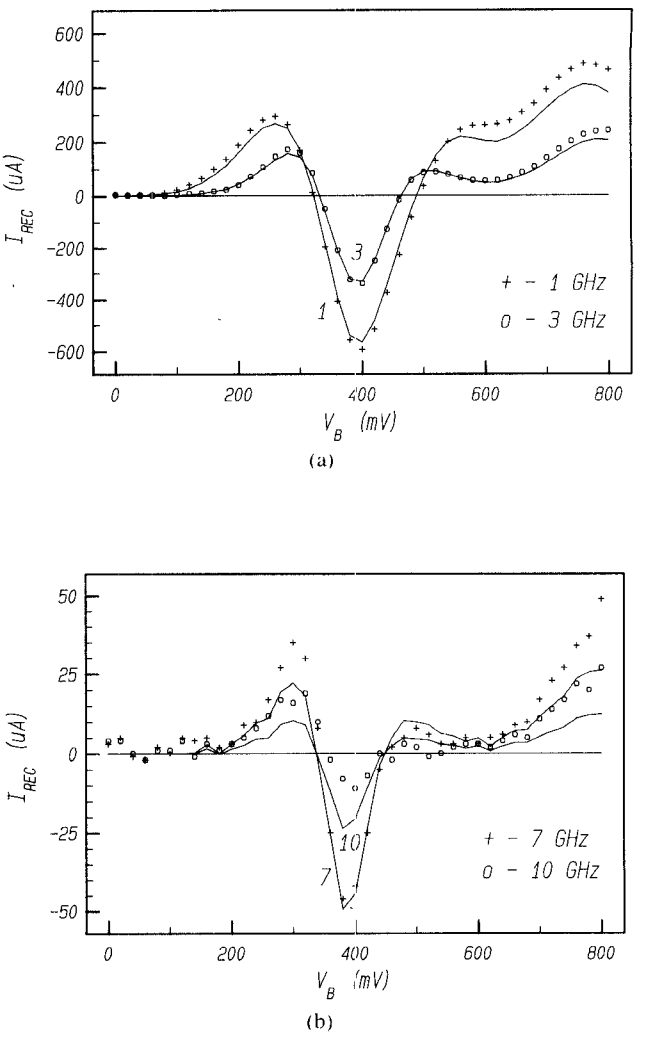

Fig. 4. Measured (symbols) and calculated (solid curve) rectified currents for a generator power of 100 μW. (a) Generator frequencies of 1 GHz (plus signs) and 3 GHz (circles). (b) Generator frequencies of 7 GHz (plus signs) and 10 GHz (circles). The solid curves are labeled with their frequency in GHz.

shunted by the capacitor (C) (see Fig. 2(c)). For a constant source power, increasing the frequency of the source reduces the voltage V_1. As the rectified current decreases, the error in its measurement increases since it is the difference between two currents which are getting closer together, I_0 and I_B. With an ammeter accuracy of ± 5 μA, small errors in I_0 and I_B lead to much larger percentage errors in I_{REC}. Overall, the four sets of results are in good agreement with one another, apart from the measurement inaccuracy at very low rectified current levels.

IV. Harmonic Analysis

Combining the S parameters of the cables, bias tee, and C-3 package network with the S parameters of the two-port formed by the parasitic elements of the RTD, the Thevenin equivalent voltage source presented to the active element (G) can be determined for the ac part of the detector circuit at the fundamental and harmonic frequencies. The dc bias circuit is independent of the ac circuit, and the bias voltage is tracked to hold it constant across the RTD. The

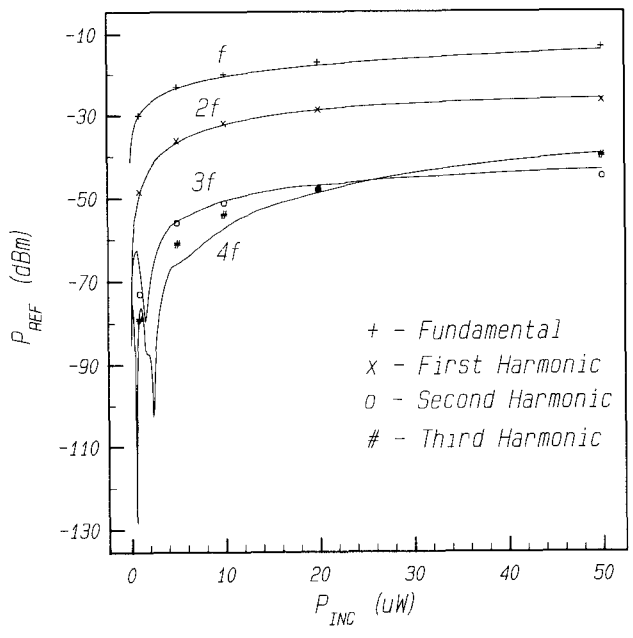

Fig. 5. Measured (symbols) and calculated (solid curve) reflected power at the fundamental and first three harmonic frequencies from an $f = 0.5$ GHz incident signal. The solid curves are labeled by frequency.

total voltage across the active element (G) is then

$$v(t) = V_B + V_1 \cos \omega t + V_2 \cos 2\omega t + \cdots \tag{6}$$

with a resulting current Fourier series

$$i(t) = I_0 + I_1 \cos \omega t + I_2 \cos 2\omega t + \cdots. \tag{7}$$

An iterative approach was taken to achieve the harmonic balance

$$V_{\text{th}}(n\omega) = Z_{\text{th}}(n\omega) I_n + V_n \tag{8}$$

where V_{th} and Z_{th} are the Thevenin equivalent generator voltage and source impedance with $V_{\text{th}}(n\omega) = 0$ for $n = 2, 3, 4, \cdots$.

The 1 GHz and 3 GHz cases of Section III were analyzed in this manner using three and two harmonics, respectively. There was no perceptible change in the rectified current calculated including the effect of these harmonics to that calculated with the assumption of no harmonics. The magnitude of the voltage at each angular frequency, $n\omega$, was approximately 1/10 the magnitude of the voltage at the preceding angular frequency, $(n-1)\omega$.

To test the accuracy of the harmonic analysis, a 20 dB directional coupler was placed between the microwave source and the bias tee shown in Fig. 3(a). A 0.5 GHz signal was applied to the device with incident powers of 1, 5, 10, 20 and 50 μW with the bias voltage set at the resonance peak, $V_B = 0.4$ V. A spectrum analyzer was used to measure the reflected power at the fundamental frequency and the generated power at the first three harmonic frequencies.

Using the results of the calculation described above for a 0.5 GHz fundamental and three harmonics, the reflected and generated powers were calculated for incident powers in the range from 0 to 50 μW. Fig. 5 shows the comparison of these calculations to the measured powers. The agreement is quite good, implying that the harmonic analysis is accurately calculating the voltage and current waveforms across the RTD.

V. Reactive Detection

Unlike passive detectors, which must absorb power to detect, an NDR diode can be operated with no absorbed power. That is, under proper bias and with the real part of its impedance equal to zero, an RTD becomes a purely reactive detector which absorbs no microwave power. Stating that there is no absorbed power implies that the average power absorbed over a cycle is zero. For example, if the RTD is biased at the resonant peak, over half the cycle, the RTD is in a positive differential resistance region where the instantaneous power is absorbed, while over the other half of the cycle the RTD is in its negative differential resistance region where the instantaneous power is generated. Given the proper ac voltage swing, the power generated can compensate for the power absorbed, yielding zero net power absorbed. Thus the RTD detects the ac voltage across the diode. Referring to (5), the required condition for reactive detection is

$$r = -G_{\text{ac}} \Big/ \left(G_{\text{ac}}^2 + (\omega C)^2\right). \tag{9}$$

Thus, for $f = 1$ GHz, $C = 2.61$ pF, and $r = 0.17\ \Omega$, the required value of G_{ac} is -0.046 mS.

Using the setup described in Section IV with the 20 dB directional coupler and the spectrum analyzer to measure the reflected power from the diode and placing a short at the reference plane of the diode, the reflection gain (the negative of the return loss) was measured as the ratio of the reflected power of the diode to the reflected power of the short in addition to measuring the rectified current. The source was set at 1 GHz with an incident power on the diode of 10 μW.

Using the procedure outlined in Section III, the reflection gain can be calculated as

$$\text{Reflection Gain} = 20 \log(|\Gamma|) \tag{10}$$

where Γ is the complex reflection coefficient of the diode. Fig. 6 shows the measured and calculated values for (a) the reflection gain and (b) the rectified current. Using (5), the large-signal impedance can be calculated, and its real part is shown in Fig. 7. It is worth noting that the points where the reflection gain is zero ($V_B = 0.4$ V and $V_B = 0.63$ V) agree well with the points where the $\text{Re}(Z_D)$ is zero ($V_B = 0.4$ V and $V_B = 0.62$ V).

VI. Tangential Signal Sensitivity

To obtain a conventional measure of the detector's performance, the microwave source of Fig. 3(a) was pulse modulated with a 1 kHz, 50 percent duty cycle square wave. A 1 kΩ sampling resistor was placed in series in the bias circuit in place of the ammeter with a differential input oscilloscope to measure the voltage across the sampling resistor caused by the rectified current. The bias voltage was set at 0.4 V with the voltage sense of the

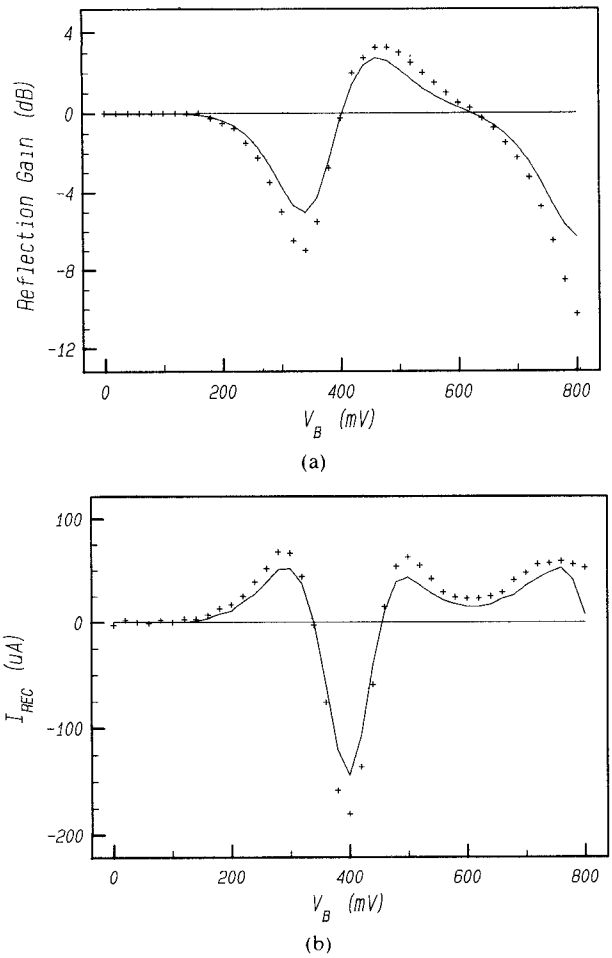

Fig. 6. Measured (symbols) and calculated (solid curve) (a) reflection gain and (b) rectified current versus bias voltage for a 1 GHz signal with an incident power of 10 μW on the diode.

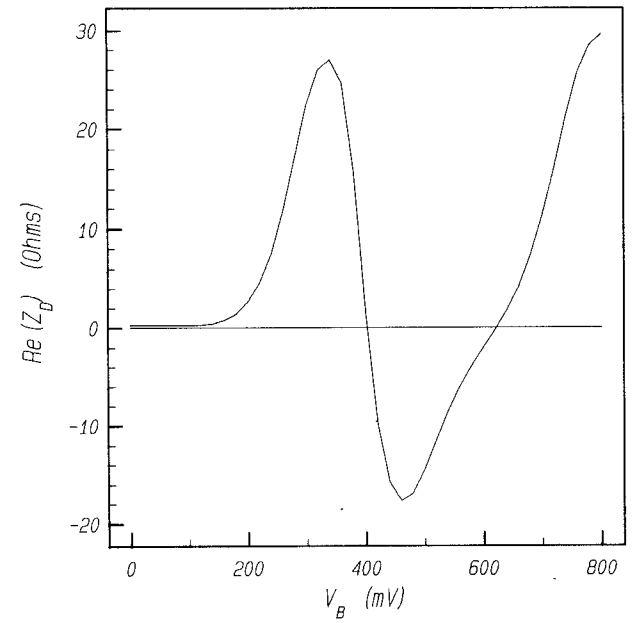

Fig. 7. Real part of the large-signal diode impedance versus bias voltage for a 1 GHz signal with an incident power of 10 μW on the diode.

TABLE I
TANGENTIAL SIGNAL SENSITIVITY (TSS) OF THE RESONANT TUNNELING DIODE AT SEVERAL SOURCE FREQUENCIES

f (GHz)	TSS (dBm)
0.5	55.5
1.0	53.5
10.0	31.5
11.0	31.5
12.0	35.0

tracking dc power supply placed on the device side of the sampling resistor so that the bias voltage would not be affected by the sampling resistor. The microwave source power was then reduced until the height of the detected voltage square wave was equal to the noise level on the oscilloscope. The RTD was then replaced with the spectrum analyzer, and the incident power was measured. The tangential singnal sensitivity (TSS), the negative of the incident power given in dBm, is given in Table I for several source frequencies.

Although the TSS of the RTD is good in comparison to commercially available detectors at the low frequencies, the RTD's TSS falls off rapidly at higher frequencies because of the device parasitics and excessive package parasitics and because no attempt has been made to maximize the ac voltage across the RTD with a matching network. Also, the RTD's detector performance can be improved by using a device with a higher peak current and a sharper peak in its $I-V$ curve. Such devices are available; however, they are harder to keep stable in and near the NDR region.

VII. MATCHING THE DETECTOR TO A SOURCE

The RTD can be matched to a source using an ideal transformer and a series reactance which can be modeled by an equivalent tee network as shown in Fig. 8. The voltage across the diode, V_D, is equal to

$$V_D = X_1 |Z_D| V_G / \left(R_0 R_D + X_1^2\right). \tag{11}$$

When R_D is negative, the maximum sensitivity for the detector will occur at the oscillation condition, $X_1^2 = -R_0 R_D$. When R_D is positive, the maximum sensitivity occurs at the condition for maximum power transfer, that is, when the impedance seen by the RTD is Z_D^*.

The detection procedure described in this paper is not new but is related to the procedures using regenerative detectors. Essentially the three-terminal triode is being replaced by a two-terminal RTD in the detection circuit.

VIII. CONCLUSIONS

We have demonstrated the microwave detection of a resonant tunneling diode with an analysis based on the diode's small-signal equivalent circuit. Although the diode is nonlinear and an incident signal will generate harmonic currents and voltages, the diode's rectified current and

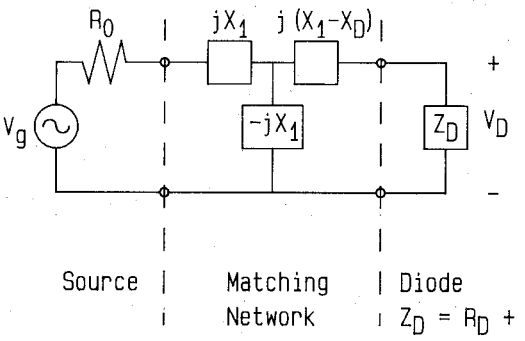

Fig. 8. Tee equivalent circuit for the voltage maximizing matching network with a matched source and the diode.

large-signal impedance can be calculated quite accurately assuming a single sinusoidal voltage is impressed on the diode at the fundamental frequency of the incident signal. Improvements in the RTD's detector performance can be made through the use of a better packaging circuit with fewer parasitics and some detector matching, as well as through the choice of better resonant tunneling structures.

A resonant tunneling diode biased at its resonant peak is expected to be an inherently better detector than a conventional Schottky barrier diode, since the resonant tunneling diode implements a full-wave rectification of an incident signal versus the at best half-wave rectification of the Schottky diode. Although we have not analyzed the noise properties of an RTD detector, we feel it should not be significantly worse than a Schottky diode biased for its maximum sensitivity to negate the improvement in the rectified signal.

Acknowledgment

The authors are indebted to Prof. P. W. Klock for the use of an HP 8510 network analyzer and his help in making the *S* parameter measurements. Colleagues D. A. Crim, Y. Zhang, and J. R. Kessler were a source of many helpful discussions in the course of this work. Prof. H. Morkoc and members of his group, J. Chen and W. Kopp, have provided invaluable service in growing and fabricating the diodes. The authors have benefited from industrial interaction with J. Broerman, C. Whitsett, and D. Ames of the McDonnell–Douglas Corporation.

References

[1] R. Tsu and L. Esaki, "Tunneling in a finite superlattice," *Appl. Phys. Lett.*, vol. 22, pp. 562–564, 1 June 1973.

[2] L. L. Chang, L. Esaki and R. Tsu, "Resonant tunneling in semiconductor double barriers," *Appl. Phys. Lett.*, vol. 24, pp. 592–595, 15 June 1974.

[3] T. C. L. G. Sollner, W. D. Goodhue, P. E. Tannewald, C. D. Parker, and D. D. Peck, "Resonant tunneling through quantum wells at frequencies up to 2.5 THz," *Appl. Phys. Lett.*, vol. 43, pp. 588–590, 15 Sept. 1983.

[4] T. J. Shewchuk, P. C. Chapin, P. D. Coleman, W. Kopp, R. Fisher, and H. Morkoc, "Resonant tunneling oscillations in a GaAs-$Al_xGa_{1-x}As$ heterostructure at room temperature," *Appl. Phys. Lett.*, vol. 46, pp. 508–510, 1 Mar. 1985.

[5] D. D. Coon and H. C. Liu, "Frequency limit of double barrier resonant tunneling oscillators," *Appl. Phys. Lett.*, vol. 49, pp. 94–96, 14 July 1986.

[6] J. M. Gering, D. A. Crim, D. G. Morgan, P. D. Coleman, W. Kopp, and H. Morkoc, "A small-signal equivalent circuit model for GaAs–$Al_xGa_{1-x}As$ resonant tunneling heterostructures at microwave frequencies," *J. Appl. Phys.*, vol. 61, pp. 271–276, 1 Jan. 1987.

[7] E. R. Brown, T. C. L. G. Sollner, W. D. Goodhue, and C. D. Parker, "Fundamental oscillations up to 200 GHz in a resonant tunneling diode," presented at the 1987 Device Res. Conf., Santa Barbara, CA, June 22–25, 1987.

[8] W. R. Frensley, "Quantum transport calculation of the small-signal response of a resonant tunneling diode," *Appl. Phys. Lett.*, vol. 51, pp. 448–450, 10 Aug. 1987.

[9] A. V. Eastman, *Fundamentals of Vacuum Tubes*. New York: McGraw-Hill, 1937, ch. 9.

[10] M. D. Montgomery, "The tunnel diode as a highly sensitive microwave detector," *Proc. IRE*, vol. 49, pp. 826–827, Apr. 1961.

[11] R. G. Owens and D. Cawsey, "Microwave equivalent-circuit parameters of Gunn-effect-device packages," *IEEE Trans. Microwave Theory Tech.*, vol. MTT-18, pp. 790–798, Nov. 1970.

[12] M. E. Hines, "High-frequency negative-resistance circuit principles for Esaki diode applications," *Bell Syst. Tech. J.*, vol. 39, pp. 477–513, May 1960.

[13] G. Gonzalez, *Microwave Transistor Amplifiers — Analysis and Design*. Englewood Cliffs, NJ: Prentice-Hall, 1984.

Joseph M. Gering (S'83) was born March 25, 1962, in Louisville, KY. He received the B.S. degree (with highest honors) in 1984 from the University of Louisville, and the M.S. degree in 1985 from the University of Illinoise at Urbana-Champaign, where he is currently pursuing the Ph.D. degree in the field of high-frequency semiconductor devices.

Mr. Gering is a member of the Tau Beta Pi, Eta Kappa Nu, and Sigma Pi Sigmas honor societies and of the Sigma Xi scientific research society.

✠

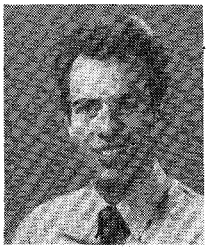

Thomas J. Rudnick received the B.S. degree in electrical engineering from the University of Illinois in 1986 (with highest honors). He was awarded a University fellowship and is currently working towards the Ph.D. degree.

✠

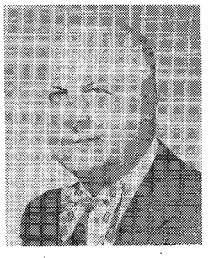

Paul D. Coleman (A'45–M'55–F'62–LF'84) received the B.A. degree in 1940 and an honorary D.Sc. degree in 1978 from Susquehanna University, the M.S. degree in physics in 1942 from Penn State University, and the Ph.D. degree in physics from MIT in 1951. He came to the University of Illinois in 1951, where he established the Electro-Physics Laboratory and became a professor of electrical and computer engineering.

From 1942 tp 1951 he was with the U.S. Air Force, first at Wright Field, Dayton, OH, and then with the Cambridge Air Research Center, where he was engaged in studies of broad-band aircraft antennas, impedance matching, and millimeter waves. At Illinois, Professor Coleman has pursued megavolt electronics and electron beam coupling processes (i.e., Cerenkov radiators), harmonic generation of millimeter waves, millimeter-wave techniques, molecular and chemical lasers, nonlinear optics, far IR optical properties of materials, and, recently, heterojunction semiconductor devices for the millimeter range.

Dr. Coleman is a Fellow of APS and a Fellow of OSA. He was on the founding committee of MTT in 1952, has been the chairman of the IEEE Quantum Electronics Council, an Associate Editor of IEEE JOURNAL OF QUANTUM ELECTRONICS, and has received the IEEE Centennial Medal in 1984. He has directed nearly 100 Ph.D. and M.S. student theses while at Illinois and has published over 100 papers in refereed journals. Dr. Coleman has been treasurer of IEEE DRC for the past 20 years.